JOURNAL OF SOLID STATE CHEMISTRY 78, 117–125 (1989)

Lattice Vibration Spectra

XLVIII. Infrared and Raman Studies of Spinel-Type Fast Ionic Conductors Li_2MCl_4 (M = Mg, V, Cr, Mn, Fe, Co, Zn, Cd) and Li_2MnBr_4

K. WUSSOW, H. HAEUSELER, P. KUSKE, W. SCHMIDT, AND H. D. LUTZ

Universität Siegen, Anorganische Chemie, Postfach 101240, D-5900 Siegen, Federal Republic of Germany

Received April 28, 1988; in revised form August 29, 1988

The Raman and infrared reflection spectra of the spinel-type halides $Li_2M^{II}Cl_4$ (M^{II} = Mg, V, Cr, Mn, Fe, Co, Zn, Cd) and Li_2MnBr_4 including Kramers–Kronig analyses and oscillator-fit calculations are presented. These results are discussed in terms of (i) fast ionic conductivity, (ii) cation distribution, i.e., normal (Li_2ZnCl_4) and inverse spinels, 1:1 ordering of Li and M^{II} in the octahedral sites (Li_2CoCl_4), (iii) phase transitions to an ordered ($LiVO_2$ type) and disordered NaCl defect structure, and (iv) two-mode behavior of the phonon modes.

Introduction

Ternary lithium chlorides and bromides with spinel structure have been reported as fast lithium ion conductors ((*1–8*) and references cited therein). Recent studies (*7*) revealed that this is true for Li_2MCl_4 (M = Mg, V, Cr, Mn, Fe, Co, Cd) and Li_2MBr_4 (M = Mn, Cd), but not for Li_2ZnCl_4. This different behavior is a consequence of the distribution of the lithium ions in the structure (inverse or normal spinels) and should reflect in the infrared and Raman spectra of these compounds. Furthermore the vibrational spectra should give information about the diffusion processes and the lattice sites involved in the ionic motion.

We therefore recorded both the far-infrared reflection spectra and Raman spectra of Li_2MCl_4 (M = Mg, V, Cr, Fe, Co, Zn, Cd) and Li_2MnBr_4 at various temperatures (150–770 K). From the reflection spectra we calculated the dispersion functions of the dielectric and optic constants including the high-frequency conductivities with the aid of the classical oscillator-fit method and Kramers–Kronig analyses. Apart from conventional infrared spectra (paraffin mulls), which show only one broad absorption, and Raman spectra of Li_2MCl_4 (M = Mg, Mn, Fe, Cd) (five scattering peaks) (*1*), no IR and Raman data have been reported in the literature to date.

Experimental Methods

The spinel-type chlorides were prepared (*1, 9*) by fusing the binary compounds in evacuated sealed borosilicate glass ampoules. The ternary chlorides are extremely hygroscopic and partly sensitive to oxygen. They must be handled under a dry Argon atmosphere.

Specimens for far-infrared measurements

0022-4596/89 $3.00

were prepared as pellets with mirror-like surfaces by pressing the powdered samples at 750 MPa using highly polished pistons. The densities of the pellets reached as much as 95% of the values calculated from the lattice constants. The IR reflectivities of specimens of the binary chlorides LiCl and NaCl prepared in the same manner were in good agreement with single-crystal data reported in the literature (*10*). The spectra were recorded at near normal incidence using a Bruker IFS 114 Fourier transform interferometer (reference: Al mirror, resolution <4 cm^{-1}). For low- and high-temperature measurements the samples were mounted on the heat exchanger of a cryostat (Cryovac, Siegburg, FRG).

The FIR reflection spectra were converted into the dielectric dispersion relations by both classical oscillator-fit methods and Kramers–Kronig analyses. Details are given elsewhere (*11, 12*). The high-frequency conductivities $\sigma(\omega)$ were computed using the relation: $\sigma(\omega) = \varepsilon_0 \cdot \omega \cdot \varepsilon''(\omega)$ (*13*) with ε_0 as the permittivity of a vacuum and ε'' as the imaginary part of the dielectric constant.

The Raman spectra, with samples taken in sealed glass capillary tubes, were recorded on a Dilor OMARS 89 multichannel Raman spectrograph with the usual right-angle geometry (spectral slit width <4 cm^{-1}). For excitation the 514.5 nm line of an Ar^+ ion laser was employed (laser power at the sample was about 150 mW). The integration time was 1–30 sec; the number of accumulations was 30–50. High-temperature measurements were performed by means of a furnace, which was equipped with quartz windows.

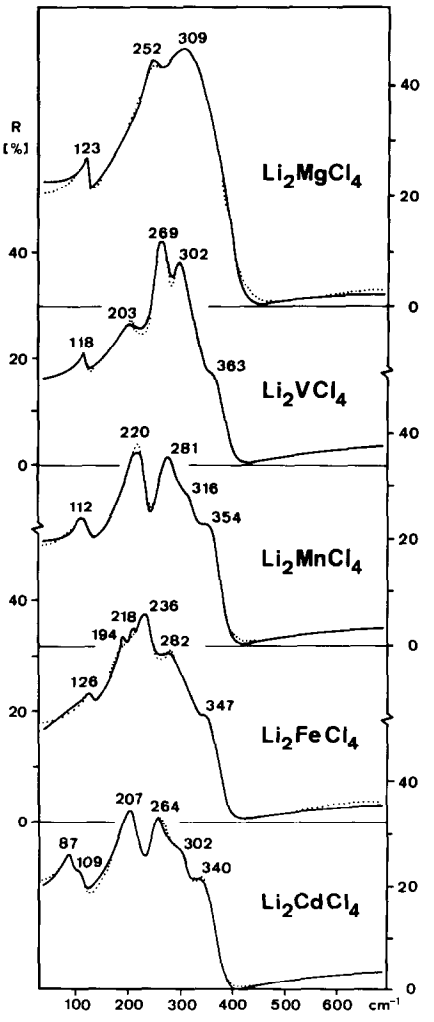

FIG. 1. FIR reflection spectra of the inverse spinels Li_2MCl_4 (M = Mg, V, Mn, Fe, Cd) at ambient temperature: dotted lines, oscillator-fit calculations; numbers, maxima of Reststrahlen bands (cm^{-1}).

Results

The FIR reflection spectra of the spinels Li_2MCl_4 (M = Mg, V, Mn, Fe, Zn, Cd) reveal up to six Reststrahlen bands (see Figs. 1–3 and Table I), which is more than the four modes of species F_{1u} predicted by group theory (*14*). The frequencies of the transversal (TO) and longitudinal optical (LO) zone center phonon modes (see Table I) were taken from the peak maxima of the $\mathrm{Im}(\hat{\varepsilon})$ and $-\mathrm{Im}(1/\hat{\varepsilon})$ dispersion relations (and from peak maxima and peak minima of the so-called modulus $|\hat{\varepsilon}| = (\varepsilon'^2 + \varepsilon''^2)^{1/2}$), respectively (see Fig. 2). The Raman spectra of most compounds (see Fig. 4 and Ta-

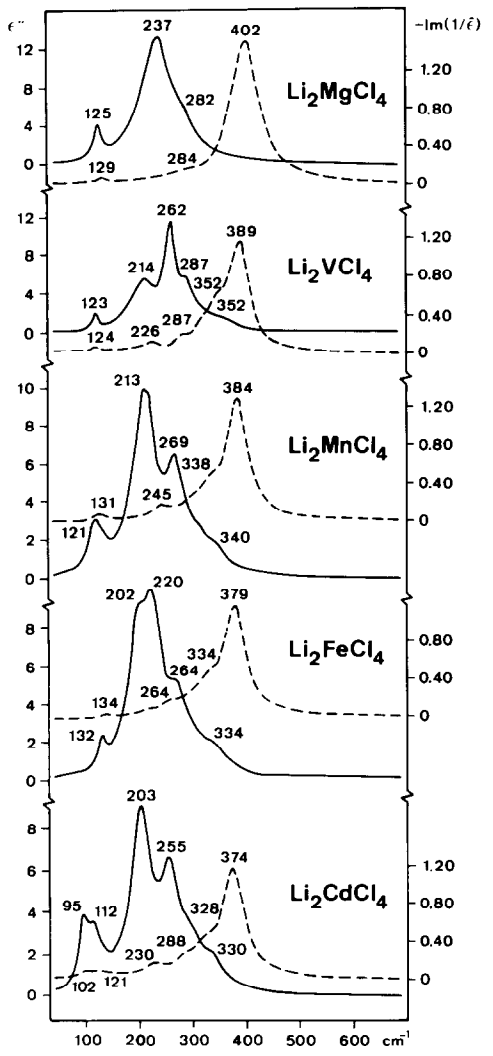

FIG. 2. Dispersion functions ε'' (= Im($\hat{\varepsilon}$)) (—) and $-\mathrm{Im}(1/\hat{\varepsilon})$ (---) of the dielectric constants of the inverse spinels Li_2MCl_4 (M = Mg, V, Mn, Fe, Cd) at ambient temperature calculated by the oscillator-fit method.

ble II) exhibit five bands in accordance with the result of a group theoretical treatment ($1A_{1g}$, $1E_g$, and $3F_{2g}$). However, from the appearance of the spectra, the compounds can be derived into three groups: (i) Li_2MCl_4 (M = Mg, Mn, Fe, Cd), (ii) Li_2ZnCl_4, and (iii) Li_2CrCl_4, Li_2CoCl_4, and Li_2MnBr_4.

The infrared and Raman studies performed at elevated temperatures (see Figs. 5–7) indicate that the Reststrahlen bands and Raman scattering peaks broaden strongly with increasing temperature. Some bands disappear, even at temperatures below the order–disorder phase transition to the NaCl defect structure polymorphs (*1*). The low-frequency region of the spectra is dominated by an increase of reflectivity and scattering intensity, respectively.

Discussion

1. Inverse and Normal Halide Spinels

From neutron diffraction studies (*4, 15*) it was revealed that the chloride spinels Li_2MCl_4 (M = Mg, V, Mn, Fe, Cd) possess an inverse cation distribution. The same structure was proposed for the other compounds of this series (M = Cr, Co) (*5, 6*) and the lithium bromide spinels Li_2MBr_4 (M = Mn, Cd) (*2*). This is supported by the Raman spectra of these halides in the present investigation (see Fig. 4 and Table II).

The most intense high-energy band of these chlorides at 246–248 cm^{-1} is obvi-

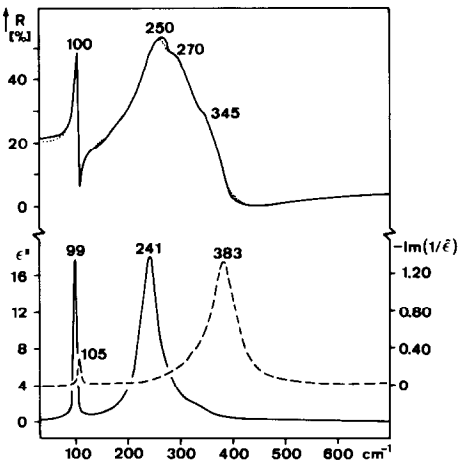

FIG. 3. FIR reflection spectrum (—), oscillator-fit calculation (···), and dispersion functions ε'' (—) and $-\mathrm{Im}(1/\hat{\varepsilon})$ (---) of the dielectric constant of the normal type spinel Li_2ZnCl_4 at ambient temperature.

TABLE I

OSCILLATOR PARAMETERS, TO AND LO PHONON FREQUENCIES (cm^{-1}) OF LITHIUM CHLORIDE SPINELS AT 150 K (DATA TAKEN FROM PEAK MAXIMA OF THE DISPERSION RELATIONS OF THE IMAGINARY PART OF THE DIELECTRIC CONSTANT ε'', THE DIELECTRIC LOSS FUNCTION $-\mathrm{Im}(1/\hat{\varepsilon})$, AND THE MODULUS $|\hat{\varepsilon}|$ OBTAINED BY OSCILLATOR FIT CALCULATIONS (OF) AND KRAMERS–KRONIG ANALYSES (KKA), RESPECTIVELY)

				ω_{TO}				ω_{LO}			
				ε''		$\lvert\hat{\varepsilon}\rvert$		$-\mathrm{Im}(1/\hat{\varepsilon})$		$\lvert\varepsilon\rvert^a$	
j	$4\pi\rho_j$	ω_j	γ_j	OF	KKA	OF	KKA	OF	KKA	OF	KKA
					Li_2VCl_4						
1	0.246	122.7	21.4	123	122	116	119	126	124	132	129
2	1.650	216.0	72.4	216	214	198	200	231	229	234	233
3	0.754	265.5	24.7	265	267	263	263	289	291	289	291
4	0.293	298.7	30.0	295	298	295	298	328[b]	330[b]	—	330[b]
5	0.132	329.8	51.7	—	330[b]	—	330[b]	355	364[b]	357	264[b]
6	0.073	369.6	38.2	362[b]	364[b]	362	364[b]	389	392	396	399
$\varepsilon_\infty = 2.78$											
					Li_2MnCl_4						
1	0.295	118.0	14.2	119	121	113	112	123	123[b]	128[b]	130[b]
2	0.474	134.6	26.6	132	131	128[b]	130[b]	137	133	145	140
3	1.985	220.0	30.3	220	222	215	214	246	246	247	248
4	0.807	274.7	27.5	274	277	273	275	308[b]	316[b]	312[b]	312[b]
5	0.361	315.3	54.3	310[b]	316[b]	312[b]	312[b]	346[b]	346[b]	346[b]	344[b]
6	0.121	353.6	35.5	346[b]	344[b]	346[b]	344[b]	393	394	398	398
$\varepsilon_\infty = 2.90$											
					Li_2CdCl_4						
1	0.628	93.0	18.6	93	95	87	87	99	103[b]	106[b]	110[b]
2	0.691	114.5	29.5	112	113	106[b]	110[b]	118	119	126	126
3	2.073	206.4	32.0	206	208	201	202	231	232	233	234
4	1.027	259.7	32.7	259	261	257	260	294[b]	292[b]	294[b]	292[b]
5	0.333	300.3	39.0	294[b]	292[b]	294[b]	292[b]	332[b]	334[b]	334[b]	334[b]
6	0.197	340.3	42.2	332[b]	334[b]	334[b]	334[b]	383	382	388	386
$\varepsilon_\infty = 3.05$											
					Li_2ZnCl_4						
1	0.0898	98.3	0.0407	98	98	98	98	106	106	106	106
2	0.2416	242.0	0.2292	240	240	234	238	—	263[b]	—	—
3	0.0064	295.9	0.0874	292[b]	290[b]	—	—	294[b]	291[b]	—	—
4	0.0053	346.1	0.1529	340[b]	335[b]	—	—	369	369	377	381
$\varepsilon_\infty = 2.96$											

[a] From peak minima.
[b] From inflections of the dispersion curves.

ously due to the A_{1g} mode, which is mainly a breathing vibration of the tetrahedral units of the spinel structure; i.e., only the halide ions move (*14*). The A_{1g} phonon mode is affected by the nature of both the anions and the tetrahedrally coordinated metal ions (*16*). The findings that this band appears at nearly constant wavenumbers in almost all compounds, therefore, confirm that the cation distribution is inverse; i.e., half of the lithium ions occupy tetrahedral 8a sites.

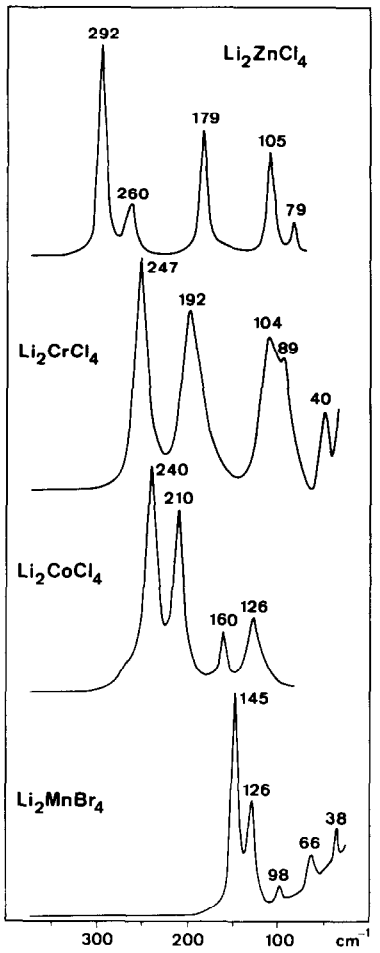

FIG. 4. Raman spectra of Li_2ZnCl_4 (normal spinel), Li_2CrCl_4, Li_2CoCl_4, and Li_2MnBr_4 (inverse spinels with superstructure ordering in the octahedral 16d sites) at ambient temperature (see Table II).

The respective A_{1g} band of Li_2ZnCl_4 is shifted to 292 cm^{-1} (see Fig. 4), indicating that Li_2ZnCl_4 has a normal cation distribution with zinc in the tetrahedral sites forming stronger bonds to chloride ions than lithium. Similar band frequencies were observed in other salts and aqueous solutions of $ZnCl_4^{2-}$ ions (*17, 18*). The other Raman modes (see Fig. 4) and Reststrahlen bands (see Fig. 3), however, reveal that Li_2ZnCl_4 behaves like a double salt rather than a $ZnCl_4^{2-}$ coordination compound (see the discussion given in (*19*)).

The lower conductivity (two to three orders of magnitude) of the zinc compound (*7*) compared to those of the inverse chloride spinels leads to the conclusion that in the case of inverse chloride spinels the tetrahedrally coordinated lithium ions exhibit much larger mobility than the octahedrally coordinated ones. However, contrary to these findings Catlow and Wolf (*8*) claimed very recently that both the octahedral and tetrahedral sublattices play an important role in the conduction mechanism.

2. Spinel Superstructure, 1 : 1 Ordering in Octahedral Sites

An orthorhombic ordered spinel superstructure (superlattice) has been established for Li_2CoCl_4 by X-ray methods (*6*);

TABLE II

RAMAN FREQUENCIES (cm^{-1}) OF SPINEL-TYPE $Li_2M^{II}Cl_4$ (M^{II} = Mg, Mn, Fe, Cd, Zn, Cr, Co) AND Li_2MnBr_4, AND SUZUKI-TYPE $Li_6M^{II}X_8$ COMPOUNDS AT AMBIENT TEMPERATURE

	A_{1g}[a]					Ref
			Inverse spinels			
Li_2MgCl_4	248	222	185	169		(*1*)
Li_2MnCl_4	248	227	163	102	70	(*1*)
Li_2FeCl_4	246	198	172	129	108	(*1*)
Li_2CdCl_4	248	173	152	134	97	
			Normal spinels			
Li_2ZnCl_4	292	260	179	105	79	
			Ordered inverse spinels ($Zn(LiSb)O_4$ type)			
Li_2CoCl_4	240	210	160	126		
Li_2MnBr_4	145	126	98	66	38	
Li_2CrCl_4[b]	247	192	104	89	40	
			Suzuki-type halides			
	A_{1g}[c]	F_{2g}	E_g	F_{2g}		
Li_6CoCl_8	237	209	139	111		(*22*)
Li_6MnBr_8	144	125	74	64		(*23*)

[a] Breathing mode of tetrahedral LiX_4 and $ZnCl_4$ units, respectively (*14*).

[b] True structure of the room-temperature polymorph not yet known (*5*).

[c] Symmetric stretching mode of octahedral $M^{II}X_6$ (*22*).

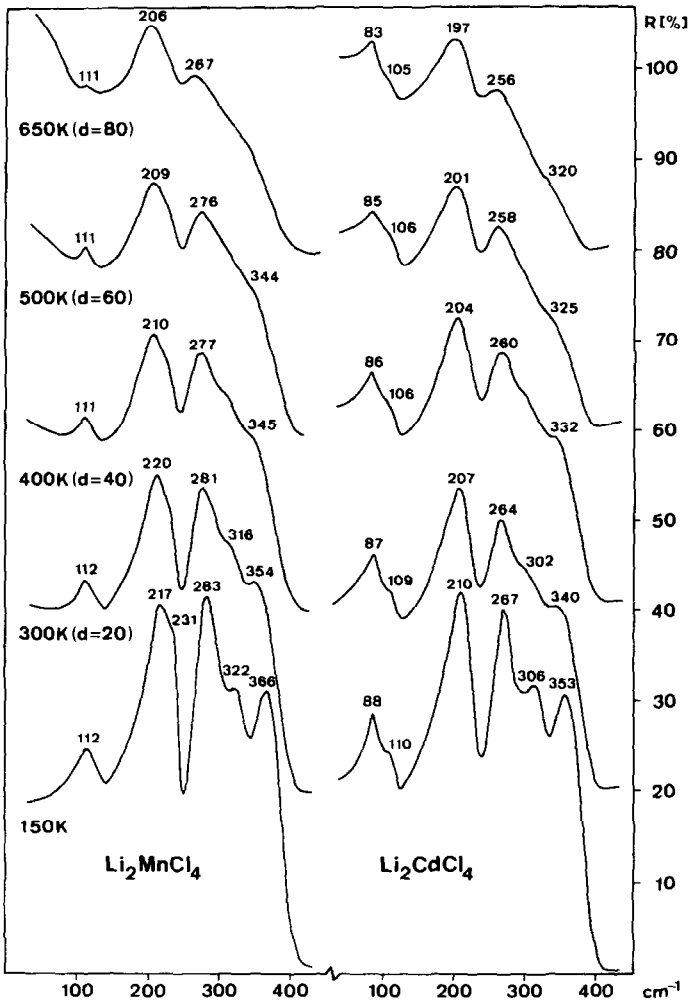

FIG. 5. FIR reflection spectra of Li_2MCl_4 (M = Mn, Cd) at various temperatures (d, shift of the ordinate scale).

for Li_2MnBr_4 a tetragonally distorted spinel structure was reported (*2*). Because the Raman spectra of these halides are very similar apart from the low-energy shift in the case of the bromide both compounds are possibly isostructural, that is, a spinel superstructure with 1 : 1 ordering (β-type, $Zn(LiSb)O_4$ (oI28) structure) of the octahedrally coordinated metal ions Li^+ and M^{2+}. A group theoretical treatment, $\Gamma = 5A_g$ (Ra) + $4A_u$ + $2B_{1g}$ (Ra) + $8B_{1u}$ (IR) + $4B_{2g}$ (Ra) + $6B_{2u}$ (IR) + $4B_{3g}$ (Ra) + $6B_{3g}$ (IR) for $\mathbf{q} \approx 0$ (*20*), of the spinel superstructure (space group *Imma*-D_{2h}^{28}) yields 15 Raman allowed and 20 IR active phonon modes, i.e., much more than observed in the spectra (see Fig. 4). This behavior, which was also observed in the case of ordered oxide spinels, is claimed to be due to the small interaction energy (or charge difference) of the metal ions in the octahedral sites (*21*). The Raman spectra of Li_2CoCl_4 and Li_2MnBr_4 are very similar to those of Suzuki-type (cF60) Li_6CoCl_8 (*22*) and Li_6MnBr_8 (*23*) (see Table II)

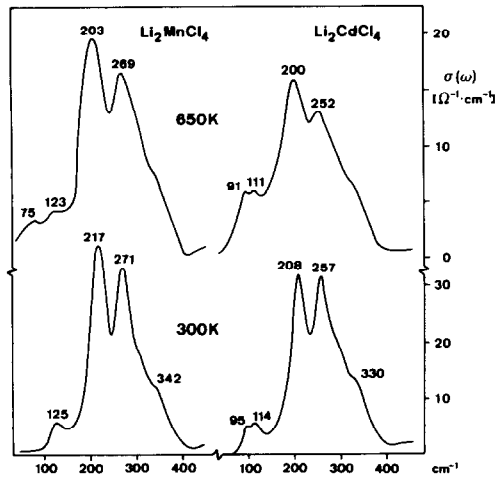

FIG. 6. Frequency dependent conductivities $\sigma(\omega)$ of spinel-type Li_2MCl_4 (M = Mn, Cd) at 300 and 650 K calculated by Kramers–Kronig analyses of the FIR reflection data.

despite the fact that in the case of the latter compounds all metal ions are in octahedral sites.

3. *Two-Mode Behavior in Inverse Spinels*

The FIR reflection spectra of inverse spinel type chlorides (see Fig. 1) reveal more details than the conventional IR absorption spectra (*1, 24*). This may partly be due to the better resolution of the Reststrahlen bands present. Additional bands found in the spectra of inverse chloride spinels, i.e., additional to the four IR allowed phonon modes of the spinel structure (see Table I), may be caused by the fact that the octahedral 16 d positions are randomly occupied by both Li^+ and M^{2+} ions and, hence, there are similar structure relations as in solid solutions. In the case of mixed crystals, additional Reststrahlen bands can be observed because of a possible two-mode behavior of the lattice modes (*25*). For the inverse sulfide spinels, e.g., MIn_2S_4 (M = Fe, Co, Ni), likewise more than four infrared active and more than five Raman allowed phonon modes are reported (*12, 16*). However, it is not fully clear whether surface or multiphonon effects, which were reported to play a role in the case of binary alkali metal halides and alkaline earth metal oxides (*26, 27*), could also be the origin of additional features in the reflection spectra obtained.

4. *TO/LO Splittings of the Phonon Modes in Chloride Spinels*

The splittings of the transversal and longitudinal optical phonon modes of the chloride spinels are relatively large as expected for salt-like compounds (see Table I and Figs. 2 and 3). The TO/LO splittings determined from the peak maxima (TO) and minima (LO) of the so-called modulus $|\hat{\varepsilon}| = (\varepsilon'^2 + \varepsilon''^2)^{1/2}$ are enlarged compared with those obtained from $\mathrm{Im}(\hat{\varepsilon})$ and $-\mathrm{Im}(1/\hat{\varepsilon})$, respectively, by up to 10 cm^{-1} (see Table I). A similar effect has been observed and discussed for sulfide spinels in (*12*). Effective dynamical charges (Szigeti charges) calculated from the TO/LO splittings are given in (*24*). The LO phonon modes of the chloride spinels are strongly coupled due to the

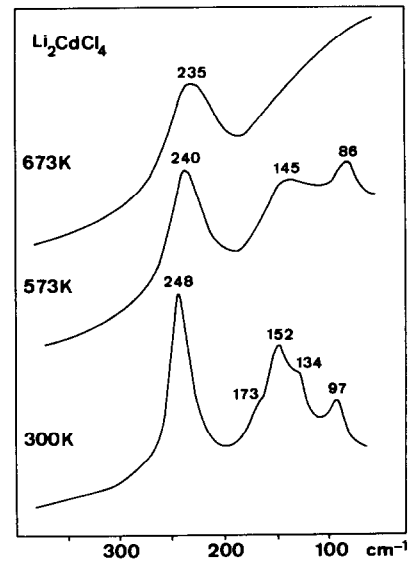

FIG. 7. Raman spectra of spinel-type Li_2CdCl_4 at various temperatures.

long-range electrostatic fields produced by these vibrations. As a result of this coupling the vibrational modes and oscillator strengths of the LO phonons largely differ from those of the respective TO phonons (see the discussion given in (*28*)).

5. Phase Transitions, NaCl Superstructure

With increasing temperature the number of the Reststrahlen bands as well as the Raman peaks decreases (see Figs. 5 and 7). Especially the high-energy bands above 300 cm^{-1} disappear. From these findings it can be concluded that the amount of tetrahedrally coordinated metal ions, which gives rise to the high-energy phonon modes, diminishes with increase in temperature. This would mean that the lithium ions migrate from the 8a sites to interstitial positions, i.e., to the normally unoccupied octahedral 16c sites. This causes a phase transition to a NaCl superstructure with 1 : 1 ordering in the octahedral voids ($LiVO_2$ (cF64) type (*29*)), i.e., with one half of the Li^+ ions occupying half of the 16c sites and the other half together with M^{2+} ions filling the 16d sites ($LiVO_2$ defect structure).

Space group and unit cell dimensions of this structure remain unchanged compared to the spinel structure and, hence, this transition is not observable in the high-temperature X-ray patterns of the ternary lithium halides (*1, 2*). However, difference thermal analyses (DTA) of Li_2CdCl_4 reveal a second endothermic peak (308°C) below the one which is due to the order–disorder phase transition to the NaCl defect structure (385°C) and which could not be interpreted in previous work (*1*). Group theoretical treatment of the $LiVO_2$-type NaCl superstructure ($\mathbf{q} \approx 0$) yields $\Gamma = A_{1g}$ (Ra) + $3A_{2u}$ + E_g (Ra) + $3E_u$ + F_{1g} + $5F_{1u}$ (IR) + $2F_{2g}$ (Ra) + $3F_{2u}$, i.e., four (instead of five (spinel)) and five (instead of four) bands allowed in the Raman and IR spectra, respectively. The high-temperature spectra reveal three Raman modes and four to five Reststrahlen bands (see Figs. 5 and 7).

6. NaCl Defect Structure

In the case of NaCl structure compounds one Reststrahlen band, but no Raman scattering peak, is expected. However, the Raman spectra of Li_2CdCl_4 (and Li_2MnCl_4) recorded at temperatures above the phase transition to the NaCl defect structure (see Fig. 7) exhibit one broad band. These findings are consistent with a disordered NaCl structure (breakdown of selection rules) with randomly distributed Li^+ and Cd^{2+} ions and vacancies in the octahedral sites.

7. Disorder-Induced Low-Frequency Modes

The FIR spectra (and to a lesser extent also the Raman spectra) recorded at elevated temperatures additionally reveal that the reflectivities (and scattering intensities) of the chloride spinels in the low-energy region increase with increasing temperature (see Fig. 5). This is obviously caused by the mobile lithium ions. In the dispersion relations, especially in that of the frequency-dependent conductivity $\sigma(\omega)$, an additional feature appears, e.g., for Li_2MnCl_4, at 75 cm^{-1} (see Fig. 6). Similar observations were made for the other compounds of this series. In the case of Li_2CdCl_4, there is a superposition with a normal phonon mode (see Figs. 5 and 6). These low-energy modes are due (after Brüesch (*30*)) to the large disorder of a fast ionic conductor. They are interpreted as approximate reaction coordinates for the jumps of the mobile ions. Likewise disorder-induced low-frequency modes were observed in a variety of fast ionic conducting materials, e.g., α-AgI (*30*).

Conclusion

The infrared reflection and Raman spectra of the spinel-type halides $Li_2M^{II}Cl_4$ and

$Li_2M^{II}Br_4$ studied reveal that (i) unlike the other halide spinels Li_2ZnCl_4 possesses a normal cation distribution, (ii) the vibrational spectra of the compounds with inverse cation distribution show a two-mode behavior, (iii) the high ionic conductivity of the inverse spinel-type halides give rise to additional low-frequency disorder-induced modes, (iv) low-temperature Li_2CoCl_4 and Li_2MnBr_4 possess spinel superstructures with 1 : 1 ordering in the octahedral sites, and (v) there are phase transitions to a NaCl superstructure ($LiVO_2$ type) additional to those to a NaCl defect structure with randomly distributed metal ions reported previously. The gradual migration of the lithium ions from the tetrahedral to empty octahedral sites connected with these phase transitions exhibit the high mobility of the tetrahedrally coordinated Li^+ ions in the inverse spinel-type halides and, hence, the fast ionic conductivity of these compounds.

Acknowledgments

The authors thank Cand. Chem. A. Pfitzner and R. Winchenbach for experimental help and the Deutsche Forschungsgemeinschaft and the Fonds der Chemischen Industrie for financial support.

References

1. H. D. Lutz, W. Schmidt, and H. Haeuseler, *Z. Anorg. Allg. Chem.* **453,** 121 (1979).
2. H. D. Lutz, H. Schmidt, and H. Haeuseler, *Naturwissenschaften* **68,** 328 (1981).
3. W. Schmidt and H. D. Lutz, *Ber. Bunsen-Ges. Phys. Chem.* **88,** 720 (1984).
4. J. L. Soubeyroux, C. Cros, Wang Gang, R. Kanno, and M. Pouchard, *Solid State Ionics* **15,** 293 (1985).
5. H. D. Lutz, P. Kuske, and K. Wussow, *Naturwissenschaften* **73,** 623 (1986).
6. R. Kanno, Y. Takeda, A. Takahashi, O. Yamamoto, R. Suyama, and M. Koizumi, *J. Solid State Chem.* **71,** 196 (1987).
7. H. D. Lutz, P. Kuske, and K. Wussow, *Solid State Ionics,* in press.
8. C. R. A. Catlow and M. L. Wolf, *Proc. R. Soc. London Ser. A* **413,** 201 (1987).
9. H. D. Lutz, K. Wussow, and P. Kuske, *Z. Naturforsch. B* **42,** 1379 (1987).
10. M. Hass, *J. Phys. Chem. Solids* **24,** 1159 (1963); *Phys. Rev.* **117,** 1497 (1960).
11. D. M. Roessler, *Brit. J. Appl. Phys.* **17,** 1313 (1966).
12. H. D. Lutz, G. Wäschenbach, G. Kliche, and H. Haeuseler, *J. Solid State Chem.* **48,** 196 (1983).
13. K. Funke and A. Jost, *Ber. Bunsen-Ges. Phys. Chem.* **75,** 436–441 (1971).
14. H. D. Lutz, *Z. Naturforsch. A* **24,** 1417 (1969).
15. C. J. J. van Loon and J. de Jong, *Acta Crystallogr. Sect. B* **31,** 2549 (1975).
16. H. D. Lutz, W. Becker, B. Müller, and M. Jung. *J. Raman Spectrosc.,* in press.
17. A. Agarwal, M. B. Patel, M. Pal, and H. D. Bist, *Spectrochim. Acta A* **40,** 1063 (1984).
18. H. Kanno and J. Hirashi, *J. Raman Spectrosc.* **9,** 85 (1980).
19. J. Preudhomme and P. Tarte, *Spectrochim. Acta A* **28,** 69 (1972).
20. J. Preudhomme, *Ann. Chim.* **9,** 31 (1974).
21. V. G. Keramidas, B. A. DeAngelis, and B. White, *J. Solid State Chem.* **15,** 233 (1975).
22. H. D. Lutz, P. Kuske, and K. Wussow, *Z. Anorg. Allg. Chem.* **553,** 172 (1987).
23. P. Kuske, Thesis, University of Siegen (1988).
24. K. Wussow, Thesis, University of Siegen (1987).
25. A. S. Barker and A. J. Sievers, *Rev. Mod. Phys.* **47**(Suppl. 2), 5140 (1975).
26. J. R. Ferraro, *Mater. Sci. Res.* **19,** 97 (1985).
27. J. R. Jasperse, A. Kahan, J. N. Plendl, and S.S. Mitra, *Phys. Rev.* **146,** 526 (1966).
28. H. D. Lutz, G. Schneider, and G. Kliche, *J. Phys. Chem. Solids* **46,** 437 (1985).
29. C. Chieh, B. L. Chamberland, and A. F. Wells, *Acta Crystallogr. Sect. B* **37,** 1813 (1981).
30. P. Brüesch, "Phonons: Theory and Experiments III," Springer Series in Solid State Sciences, Vol. 66, Springer-Verlag, Berlin (1987).